RATE OF VEHICLE REMOVAL FROM OFFSET INKS: a gravimetric determination of the imbibition behavior of pigmented coating structures

J. Schoelkopf[1]
Senior Scientist

P. A. C. Gane
Vice President Research & Development
Paper & Pigment Systems

C. J. Ridgway
Senior Scientist

D. C. Spielmann
Group Leader Paper Research

Omya AG
CH 4665 Oftringen, Switzerland

G. P. Matthews
Reader in Applied Physical Chemistry

Environmental and Fluids Modelling Group
Department of Environmental Sciences
University of Plymouth
PL4 8AA Devon, U.K.

ABSTRACT

This work experimentally examines the competitive rate of removal of ink vehicle from a setting commercial offset ink. The competition is established by the absorptive forces of a porous coating network acting against the progressive concentrating boundary ink film. The experiments are made gravimetrically using a compressed tablet of calcium carbonate coating pigment brought into contact with a supersource of ink. The porosities of the model substrates are determined by mercury intrusion porosimetry. Effects such as polymer and ink resin size exclusion at the interface between the ink and the surface of the porous medium are considered. Results are compared with a number of different models. A good correlation is seen with the earlier prediction of fluid loss based on observed ink tack rise on commercial offset paper using the force-time integral recorded by the SeGan Ink Surface Interaction Tester (Gane, Schoelkopf, and Matthews, 2000), where a process viscosity was treated as an uniaxial extensional viscosity, whose magnitude is a function of ink oil content. These supersource data confirm the finding from the thin film application that the weight fraction of oil lost from an ink is linear with time during the tack rise period, such that the rate oil mass lost from an ink decays according to an approximate inverse square law with time. The implications for print quality are discussed in relation to the dominance of a preferred network absorption pathway characterizing the initial tack rise regime. Control of this pathway dynamic in relation to the total pore volume is shown to be a major factor in controlling the press runnability performance of coated paper in relation to the tack build.

Keywords: ink vehicle, mineral oil, ink tack, viscosity, printability, offset printing, absorption.

[1] Author to whom correspondence should be addressed

INTRODUCTION

The imbibition of a wetting liquid into a porous structure is a frequently occurring phenomenon in both natural and industrial systems. The details of this process are only partially understood, especially when it comes to systems with some complexity in terms of pore geometry, surface energy heterogeneity and liquids which are dispersions or suspensions containing a variety of components. On the other hand, it is well known that the physical phenomena occurring during and after the application of printing ink in an offset print process are important factors in achieving the desired print properties. Ink vehicle, the continuous liquid phase, is removed from the setting film by absorption into the porous paper coating surface. The dynamics of this short-term absorption are observed as a build-up of internal ink tack, and a subsequent longer term desired decay in surface tack. Both of these effects are linked to properties of the final cured ink film, such as print gloss, press room and converting runnability and rub-resistance. The optimal control of this complete tack cycle is therefore crucial for the multicolor offset printing process.

On a printing press that has reached equilibrium, there occurs an ink split balance between the printing blanket and the tackifying ink layer(s) from the previous printing station(s). The ink retained on the blanket is itself tackified due to the pre-absorption effect on the paper. This ink is effectively tack aged. When testing the tack response of ink on paper, therefore, it is essential to realize that these long timescale aging effects are relevant, despite the short contact times between the paper and the aged, blanket-retained ink. On this account, tack must be studied in relation to the aging process. This is achieved by adopting a contact blanket material which records tack on paper over the complete tack cycle, which can last from seconds, through minutes, to, in some cases, hours.

The connection between ink tack and long timescale imbibition processes can also be supported by the fact that the driving force for absorption is the same whether the fluid front is just under the surface or deep inside a homogeneous coating structure. What changes with permeation depth is the resistance to that wetting force. By observing the change in resistance with time, i.e. the fall-off in absorption rate as fluid permeates a structure, an extrapolation can be successfully made to shorter times. This forms the basis for the study presented in this paper.

In previous studies we investigated the mechanism of absorption of pure liquids into coating pigment structures (1). We identified the relevance of inertial flow as physically predicted by Bosanquet (2) who expanded the well known Lucas-Washburn (3) equation to contain the inertial effect of the liquid mass which has to be accelerated by the wetting force. There exists a time dependent optimum for flow rate as a function of capillary radius, liquid density and viscosity. The consequence is that pores up to a given diameter in a porous network, this diameter being in turn a function of time, fill very fast while bigger features remain by-passed and tend to remain unfilled under conditions of limited supply volumes of fluid as is the case with thin applied ink films. This promotes a preferential pathway flow (4). The existence of unfilled or by-passed pores is also known from soil science and studies made using micro models (5). Inertial flow in a glass capillary was observed by Quere using a high speed camera (6). With modifications, we applied the Bosanquet equation to a sequential wetting algorithm for Newtonian fluids in a pore space simulator, Pore-Cor[2], referred to as the network simulator, further developed to include novel double cone throat geometry and described in the literature (7).

Offset inks contain Newtonian liquids such as solvents and extenders, but the rheology of the ink itself, as it interacts with the paper and the printing press, shows a complex behavior. The absorption process is also complicated further as the porous paper coating structure does not imbibe the ink itself but mainly the liquid phase, the so-called vehicle, due to size exclusion of binder/pigment particles and adsorption of solvated resins (8). This leads to an effective rise in viscosity of the ink and to a fast formation of a progressively immobilizing layer of binder and pigment particles on the coating surface. According to a model proposed by Xiang and Bousfield (9), in some cases this immobilized layer may be considered as a separate delineated filtercake structure. We found, however, that this model works well for high volume pigmented fluid inks, such as flexographic inks (10), but that it is difficult to determine the presence of a filtercake experimentally for viscous offset inks. Rather it was seen that in the case of offset printing a progressive increase in viscosity as the boundary between ink and paper is approached provided a better practical description (11).

[2] Pore-Cor is a software program of the Environmental and Fluids Modelling Group, University of Plymouth, UK.

In this work we extend the former study (11) which combined rheological methods to study the relaxation of pre-sheared ink together with direct tack measurement using the tack force-time integral formed repeatedly as a function of time as provided by the SeGan Ink Surface Interaction Tester[3] (ISIT). This approach was used to reproduce the shearing effect of ink distribution and film split on the press. The observed ink tack rise, measured as a function of time, was used to obtain a predicted volume loss of fluid from the ink by comparing this tack rise with a predetermined shear viscosity of the ink under different oil concentrations. A model was developed to describe the solids and viscous behavior of the ink under the controlled extensional acceleration conditions of the static point ISIT test, which correlated the single integrated force-time curves derived from each individual machine "pull-off", made at a given defined time after printing, with a process extensional viscosity and hence, via the Trouton ratio, to the observed relaxing shear viscosity of the ink. Following this observation we derived a predicted rate of mass loss of oil from the ink to find that this rate, to a first approximation, falls off as t^{-2}. It is the aim here to analyze this prediction further and to determine if it really is representative of the processes involved.

We use a technique described earlier which samples directly the mass uptake of fluid into a macroscopic consolidated structure of coating pigment (1). This technique was previously used to investigate uniquely the imbibition of offset oil into structures over a range of different porosities, determined independently by mercury porosimetry, adopting the required specially developed compression correction algorithms (12). The important aspect of this work is that we maintained the chemical and overall geometrical similarity of the samples - a feature much overlooked when workers have attempted to correlate absorption between different porosity samples.

OVERVIEW OF PRINT AND POST-PRINT MECHANISMS - relation to absorption models

In the offset, or lithographic print process, after the initial pressure impulse applied to both sides of the paper from the printing nip, shown by Oittinen (13) not to have an effect with respect to impressed fluid or ink, three main mechanisms become active in the tackification and setting of an offset ink. Capillary forces and diffusion plus limited evaporation later in the sequence of heatset web offset, remove the fluid phase from the applied ink layer causing a progressive concentration of solids towards the boundary between ink and the surface of the porous substrate. The curing, which is mainly oxidative, ideally occurs after the removal stage of a critical amount of fluid components, resulting in a solidification of the ink film involving polymerization and setting of resin binder components in the ink formulation.

The application of the Lucas-Washburn (LW) equation, assuming a simple bundle of capillaries, often leads to an unrealistic dimension of the effective pore radius and contradicts observation when comparing ink setting on fine gloss coating structures with those of coarser matte coatings. Furthermore, the parameters fail to scale while retaining the invariant nature of surface energy and contact angle. The classically derived equation of Bosanquet (2), which was virtually ignored for many years since its inception in 1923, includes the effect of inertial retardation of the liquid as it becomes accelerated into the larger pores. Inertia is shown to promote a short lived regime of flow that is linear with respect to time in contrast to the square root proportionality of the LW equation. While this effect in straight capillaries is detectable it was considered not to be relevant because of the short timescale of its influence, e.g. ~ 10 ns for water into a capillary of diameter ~ 0.1 µm. However, the effect in a porous network is considered to be additive. In each single feature of a porous network where the liquid is accelerated, inertia acts over a timescale similar to the pore filling time for the finer pores we encounter in paper coatings and leads to a differential in wetting front velocity and position during absorption between the finer and the larger pores. Interestingly, in experimental approaches, on a macroscopic scale, a proportionality with respect to the square root of time is observed due to mass balance criteria and systematically led to the assumed verification of Poiseuille flow and hence Lucas-Washburn dynamics with, however, the remaining need for a defined effective capillary radius or surface energy relationship to describe the discrepancy between absorption rates for fine and coarse structures. This issue is discussed further in some detail in recent publications (4), (7), (14). High liquid viscosities shift the time of inertial flow into even shorter timescales and low densities decrease the effect of inertial retardation. In the case of offset inks, where the fluid is formed from alkanes in a mineral oil fraction or vegetable oils, the viscosity is in the order of 0.5 - 40 mPas and the density in the order of 800 kgm^{-3} and this maintains the relevance of the inertial timescale during the pore selection process within the porous network of a paper coating.

[3] ISIT is a product name of SeGan Ltd, Perrose, Lostwithiel, Cornwall PL22 0JJ, U.K.

The network simulator

The network simulator is a computer model that simulates the void-space structure of porous materials. It has been used to model the structures of a wide range of porous materials including sandstones (15), medicinal tablets (16) and soil (17). It uses a unit cell with 1,000 cubic pores in a 10x10x10 array, connected by up to 3 000 throats, i.e. one connected to each cube face. Each pore is equally spaced from its neighboring pores by the 'pore row spacing' Q, and each unit cell is a cube of side length 10 Q. There are periodic boundary conditions, with each cell connected to another identical unit cell in each direction. The pore and throat size distributions of the unit cell are optimized so that the simulated percolation curve fits as closely as possible to the experimental mercury intrusion curve (18). The distributions of pore and throat sizes are characterized by two parameters, 'throat skew' and 'pore skew'. The distribution of throat sizes is log-linear. The throat skew is the percentage number of throats of the smallest size. The linear distribution pivots about its mid-point at 1 %. The pore skew increases the sizes of the pores by a constant multiple. However, the pores with the largest sizes are truncated back to the size of the largest throat, thus giving a peak at the maximum size. The positions of the pores and throats are random, determined by a pseudo-random number generator.

In a recent approach (19) the geometry of the unit cell was modified by changing the cylindrical throats to a convex double-cone construction. Such a geometry can cause a pressure hold-up of the percolation of non-wetting fluids such as mercury and a change in the speed of absorption of wetting fluids. The variations in capillary pressure and wetting speed are used reflect the combined effects of heterogeneity in both geometry and in the interaction energies between a permeating fluid and the surfaces of the voids in a natural experimental sample. This new geometry was shown to give improved absorption simulations which have a better match with absorption experiments and is the form used for the present study.

A matrix of values of throat skew and connectivity are tried, and the void structure chosen which has percolation characteristics most closely matching the experimental values. The value of Q for the chosen structure is adjusted so that its porosity matches the experimental value while ensuring that no pores overlap. It is not normally possible to represent the actual complexity of the void network of a natural sample using the relatively simple geometry of the network simulator unit cell. Also, the size of the unit cell is often smaller than the representative elementary volume (REV) of the sample. Therefore, different unit cells must be generated using different seeds for the pseudo- random number generator. The algorithm is designed so that different structural parameters in conjunction with the same seed of the pseudo-random number generator produce a family of unit cells which are similar to each other – for example all may have a group of large pores in the same region (17). Different stochastic generations use a different pseudo random number generator seed, and can either use the original network simulator optimization parameters or can be re-optimized to the experimental data. The effects of the limiting boundary conditions of the unit cell have been addressed (7). This issue means that the relevant timescale for study using the network simulator without boundary corrections is at the short times as imbibition begins and the relevance to the macroscopic experimental studies is taken as the transition occurs between the short time absorption dynamic and just before the need for boundary upscaling corrections.

Implementing the wetting algorithm

Details of the application of the algorithm are given in the earlier work (7). At the start of the imbibition calculation the total time length for the imbibition is specified. The length of a time step is 1 nanosecond, its value being such that the maximum distance advanced by the fluid in one time step is never more than 0.1 Q . The flow rate varies greatly with throat diameter and conicality, with the consequence that many millions of timesteps must be calculated. A typical calculation of imbibition to fill one fifth of the unit cell takes 20 hours on a 600 MHz personal computer.

The Bosanquet equation is used to calculate the wetting flux in each pore and throat in the void network at every time step. Once a throat is full, the volumetric flow rate of the fluid leaving the throat is calculated and this fluid starts to fill the adjacent pore. The pore can be filled by fluid from more than one throat, which may start to flow into it at different times. Once a pore is full, it starts to fill the throats connected to it that are not already full and which are not already filling from other pores. If at any stage the outflow of a pore exceeds the inflow then a mass conservation restriction is applied which removes this imbalance and restricts the fluid flow further into the network.

The imbibition is quantified as F, the fraction of the total void volume in the unit cell which is filled with the fluid at time t. For comparison with experiment, the imbibition is expressed as a Darcy distance $L = 10\ Q\ F$. This corresponds to the volume-averaged distance between the sample interface with the fluid source and the wetting front.

MATERIALS

The bulk samples used in this work are cubic blocks of pigment. We concentrate here on the use of a spray dried predispersed natural ground calcium carbonate derived from limestone with a particle size distribution of 91 wt% < 5 µm, 55 wt% < 2 µm and 30 wt% < 1µm.

The detailed method of powder compaction and subsequent sample grinding is described elsewhere (1). It proved to give a reproducible and relatively homogeneous porous structure. Such homogeneity was required so that specimens from the same sample could be used separately for the fluid imbibition and mercury porosimetry experiments. The sample was consolidated and, therefore, did not require a sample vessel for the fluid imbibition experiments, thus eliminating uncertainties of fluid interactions between the sample and such a vessel.

To reduce artifacts caused by the wetting of their outer surfaces, the samples were coated with a thin barrier line of a silicone polymer around the base of the vertical edges arising from the basal plane. The polymer was Dow Corning P4-3117 conformal coating. The remainder of the outer planes were not coated, to allow for the free movement of displaced air during liquid imbibition, and to minimize any interaction between the silicone and the absorbed liquid.

The oil used was a Haltermann PKWF 6/9 af (aromat free) quality. The contact angle of oil / calcium carbonate, θ, was assumed to be zero following the data of Chibowski and coworkers, (20), (21). This was also confirmed by observing the complete spreading of an oil droplet on a dispersant adsorbed crystal surface of calcium carbonate.

The ink used was a commercial ink, Skinnex cyan 4x73[4].

MERCURY POROSIMETRY

Each structure used for the experimentation was analyzed independently with mercury porosimetry. A Micromeritics Autopore III mercury porosimeter was used to measure the percolation characteristics of the samples. The maximum applied pressure of mercury was 414 MPa (60 000 psia), equivalent to a Laplace throat diameter of 0.004 µm. Small samples were used, each of around 1.5 g in weight. The equilibration time at each of the increasing applied pressures of mercury was set to 60 seconds. The mercury intrusion measurements were corrected for the compression of mercury, expansion of the glass sample chamber or 'penetrometer' and compressibility of the solid phase of the sample by use of the following equation from Gane, Kettle, Matthews and Ridgway (12) as incorporated in the software Pore-Comp[5], referred to as the intrusion corrector:

$$V_{\text{int}} = V_{\text{obs}} - dV_{\text{blank}} + \left[0.175(V^{1}_{\text{bulk}})\log_{10}\left(1+\frac{P}{1820}\right)\right] - V^{1}_{\text{bulk}}(1-\Phi^{1})\left(1-\exp\left[\frac{(P^{1}-P)}{M_{\text{ss}}}\right]\right) \qquad (1)$$

where V_{int} is the volume of intrusion into the sample, V_{obs} the intruded mercury volume reading, dV_{blank} the change in the blank run volume reading, V^{1}_{bulk} the sample bulk volume at atmospheric pressure, P the applied pressure, Φ^{1} the porosity at atmospheric pressure, P^{1} the atmospheric pressure and M_{ss} the bulk modulus of the solid sample. The volume of mercury intruded at the maximum pressure, once corrected for sample compression effects, can be used to calculate the porosity of the sample.

MEASURING THE ABSORPTION DYNAMIC OF LIQUIDS

The rate of liquid uptake was measured using an automated microbalance, namely a PC-linked Mettler Toledo AT460 balance with a precision of 0.1mg, capable of 2.7 measurements per second. A software program was developed (7)

[4] Skinnex is a product name of K+E Inks, Stuttgart, Germany.
[5] Pore-Comp is a software program of the Environmental and Fluids Modelling Group, University of Plymouth, PL4 8AA, U.K.

and improved further in the present work, interfacing with the balance for data sampling[6] (see appendix). To provide a sufficiently slow and precise approach of the sample down to the liquid surface, a special sample holder was constructed Fig. 1 - details are given elsewhere (7). All experimentation in this study was maintained under constant temperature conditions of 23.0 ±1.5°C.

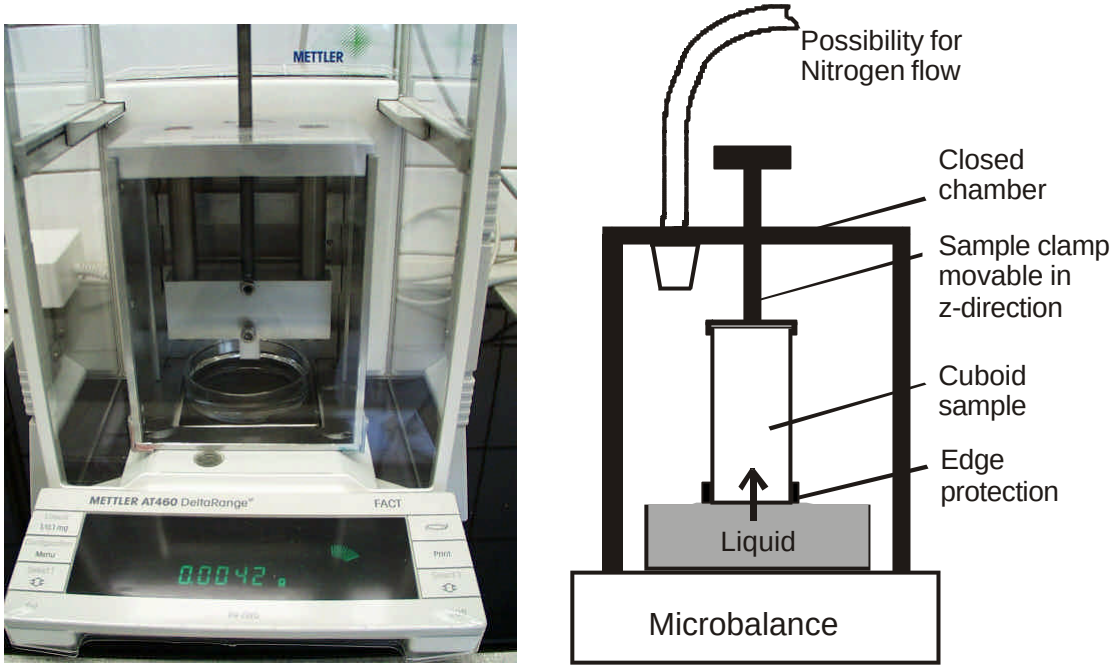

Fig. 1 Gravimetric wetting apparatus.

We start our experimentation with imbibition of the same mineral oil we used formerly in tack experimentation with diluted inks (11). For the first time it is here possible to show imbibition curves into structures over a range of different porosities, while maintaining the chemical and overall geometrical similarity of the samples. The change in porosity is dominant over the change in connectivity. This is typical in paper coatings when keeping the pigment constant and changing calendering conditions.

As previously defined (7), the total force F_{total} acting on the solid-liquid interface during the imbibition of oil into the calcium carbonate is the sum of the wetting, gravity and buoyancy forces, all of which are functions of time, t :

$$F_{total}(t) = F_{wetting}(t) + F_{gravity}(t) + F_{bouyancy}(t) \qquad (2)$$

The difference here, compared with earlier results using liquids with low and medium viscosity, is that in this work we extend the experimentation to involve both oil and an offset ink. The very high viscosity of the ink delays the hydrodynamic effects more so than in the case of pure oils and so the terms in equation 2 are ill-defined upon initial contact with the ink and special experimental techniques have to be developed to allow for the slow relaxation dynamic before the forces shown reach equilibrium. [This aspect is discussed further in the section following below.]

Preliminary trials showed that the silicone ring around the basal edge is efficient in preventing fluid from creeping up the outside of the sample, so that, to a good approximation, $F_{side} = 0$. $F_{contact}$, caused by the force of attraction around the perimeter of the meniscus pulling the liquid up towards the fixed solid, is constant for $t > t_1$, which, in the case of the viscous ink, can be significant. F_{base} is caused by the formation of the meniscus and the subsequent movement of fluid through the meniscus; the first effect is completed also in time t_1, and the second is assumed negligible because the meniscus is thin and the curvature slight compared to the total cross-sectional area of the uptake. There is also

[6] Software available from the authors.

inertia in the system which causes a lag and then an overshoot in the recorded weight. This effect is assumed to be completed in a time t_2, which is greater than t_1. Thus, to a good approximation in our experimentation,

$$\begin{aligned} &F_{\text{total}}(t > t_2) = F_{\text{wetting}}(t > t_2) \\ &= F_{\text{wi}}(t > t_2) + F_{\text{base}}(t > t_2) + F_{\text{contact}}(t > t_2) + F_{\text{side}}(t > t_2) \\ &= F_{\text{wi}}(t > t_2) + c \end{aligned} \qquad (3)$$

The constant term c can be found by fitting the function $F_{\text{total}}(t > t_2)$ with a Washburn based function, Eq 5, and extrapolating back to $t = 0$ at which point $F_{\text{wi}} = 0$. Then the constant term can be subtracted from F_{total}, and F_{wi}, the wicking force or internal wetting force, can be calculated at all times. In practice, the forces are measured as apparent changes in liquid weight. Experiments with five similar samples were shown to have a repeatability within ±0.96 % in imbibition mass at 1,000 s (7).

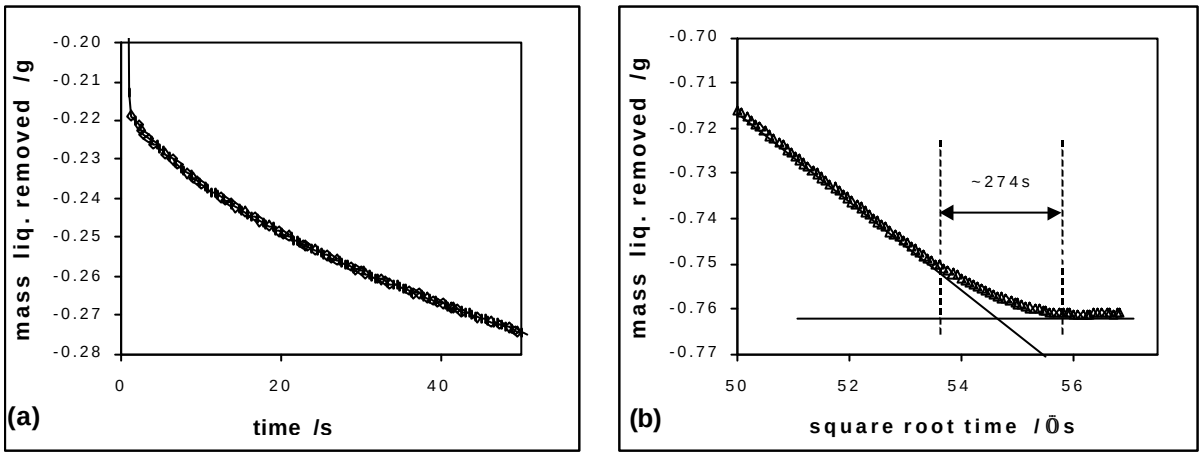

Fig. 2 *a) The absorption data for oil as detected by the balance, b) the final stage of absorption, namely the saturation of the sample. The structure shown has a porosity of 32.26 %.*

A typical absorption curve for oil, as sampled from the balance, is shown in Fig. 2a). At the very beginning, the last part of the wetting jump is visible with the subsequent regime being linear in respect to the square root of *t*. In Fig. 2b) we see the sample in the final stage of saturation where the first imbibition pathways have already reached the top of the porous sample and there is subsequent filling of slower imbibing capillaries and liquid redistribution. This phenomenon is particularly relevant when we consider limited fluid volume, such as in the case of thin ink films, as it demonstrates clearly the preferred pathway filling of the sample.

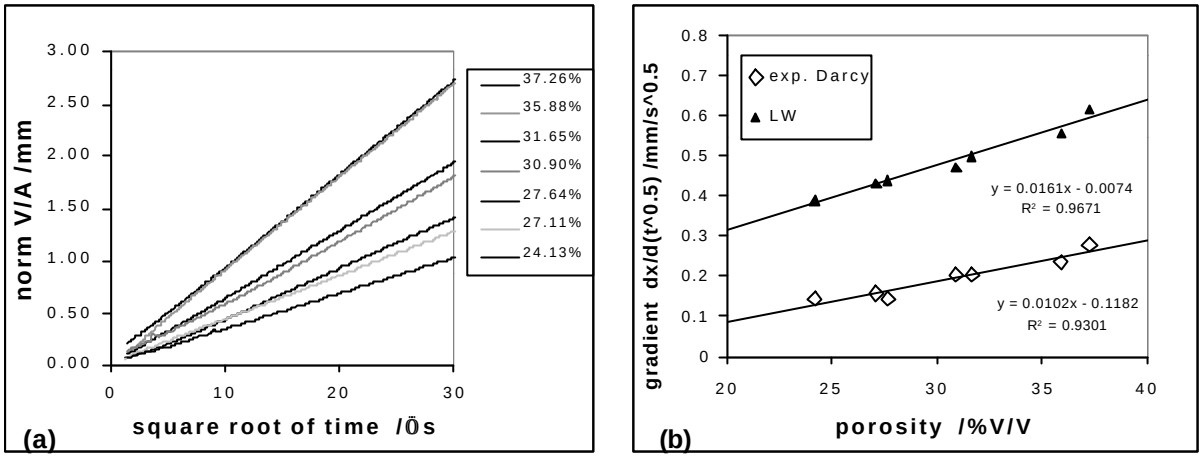

Fig. 3 *(a) imbibition curves for the different porosities normalized to [V(t=0)/A]=0, (b) the slopes of x, described as (i) experimental Darcy length and (ii) as LW-calculated, tracking with porosities.*

In Fig. 3(a) we see the macroscopical uptake, as a volume, $V(t)$, per unit area, A, with respect to the square root of t. For long times there is the expected relationship with $\sqrt{t}$ but at shorter times there is evidence of deviation, for example at 35.88 % porosity in Fig. 3(a). The mass data are normalized as described above to remove the contribution of the other forces in order that at $t = 0$, $F_{wi} = 0$. The uptake is analyzed directly as a Darcy length x,

$$x = \frac{m(t)}{\rho A \varphi_{Hg}} \qquad (4)$$

where $m(t)$ is the mass of liquid absorbed as a function of t, ρ is its density, A is the area of transplanar uptake and φ_{Hg} is the porosity found by mercury intrusion. A plot of x against the square root of time results in a similar picture as for $V(t)/A$. We compare the experimentally determined Darcy length with that predicted by the Lucas-Washburn equation Eq.5,

$$x = \sqrt{\frac{r_c \gamma_{LV} \cos\theta \; t}{2\eta}} \qquad (5)$$

where x again is the distance traveled by the liquid, γ_{LV} is the surface tension of the liquid, θ is the contact angle, η is the dynamic viscosity and r_c is the capillary radius where we used ½ of the d50-diameter which is the capillary diameter at 50 % intrusion volume of the corrected Hg-intrusion curves (12) over the diameter range of 0.004 µm and 1.22 µm. These diameters are shown in Fig. 4.

To illustrate the deviation from the predicted constant of scaling in respect to porosity given in the Lucas-Washburn model, we compare the experimental scaling of Eq. 4 with that predicted by Eq. 5 as a function of porosity. This is conveniently shown in Fig. 3(b) where we have formed the respective scaling gradients in each case as $dx/dt^{0.5}$. These were determined by a linear regression analysis to obtain the relationships shown in Fig. 3(b).

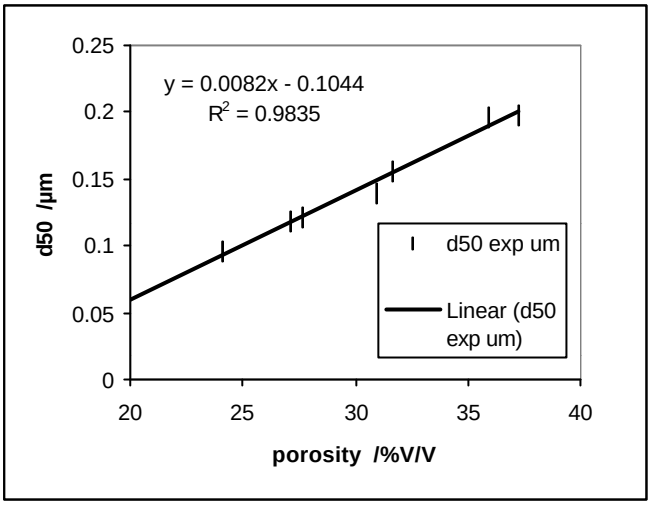

Fig. 4 The d50-diameter which is the capillary diameter at 50 % intrusion volume of the The-corrected Hg-intrusion curves as a function of porosity.

The effect of inertial wetting and the proposed pathway phenomenon are in principle not detectable using the Darcy law. This is because Darcy describes a volume uptake only which does not account for liquid distribution micromechanisms between selective pore structures. The limitation of the Darcy assumption is shown schematically in Fig. 5.

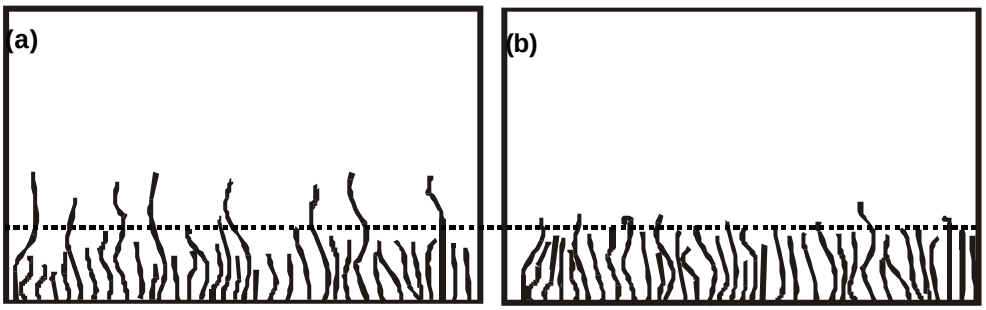

Fig. 5 *A schematic drawing, omitting interconnectivity, showing a) the preferred pathway effect and b) a more equilibrated uptake, both having the same Darcy length (dotted line).*

It is evident from Fig. 3(b) that there is a discrepancy between the experimental scaling gradients and the gradients based on calculations using the LW Eq. 5. Similar discrepancy has been reported by other workers elsewhere (22), (23). Usually it is argued that the contact angle must be changing under dynamic imbibition (24). For this case, however, this is not a valid argument as the work of Chibowsky and co-workers, (20), (21), (25), has shown that aliphatic alkanes completely wet a number of mineral surfaces including calcium carbonate. This is the basis of why these authors use alkanes to determine an effective pore radius. Only a small amount of work has been done confirming this effective radius using other methods. Other investigators (23), however, used a variety of alkanes for wicking experiments into ceramic structures. They also assumed that the contact angle was zero, and found an effective radius which was smaller than that afforded by mercury porosimetry by a factor of about 2, which corresponds well with our findings here (Fig. 3(b)). They questioned the mercury porosimetry result. Our opinion is that mercury porosimetry has shown its reliability with many structures of high bulk moduli and was confirmed also in our previous work using pressureless liquid imbibition methods (1). There is, furthermore, no argument to question the surface tension and the viscosity of the liquid as the remaining influential parameters because they can be easily measured. In previous work (1), (15) we considered other possible mechanisms such as effects of geometry,

inhomogeneous surface chemistry, meniscus retraction etc. In this context, while we have carefully maintained constant material properties, we feel that over small ranges of porosity basic geometrical changes are not likely to dominate, except perhaps in the case of connectivity, but rather the effective pore and throat size distributions. This is not meant to be exclusive but allows us to move on to explore briefly an alternative model.

If we were to challenge the Poiseuille flow assumption and use an equation of purely inertial flow, as given in our short time solution of the Bosanquet effect (7),

$$x = t\sqrt{\frac{2\,g_{\mathrm{LV}}\cos\theta}{r_{\mathrm{c}}\,\rho}} \qquad (6)$$

we would obtain non linear gradients with respect to $t^{0.5}$ for the liquid imbibition. Therefore, we propose that the linear t absorption dynamic is indeed short lived but acts to decide into which pores the fluid will flow such that the imbibing fluid can only "see" a fraction of the existing voidage of the porous sample as it selects the finer pores, but that it subsequently follows the viscous dynamic as t increases as predicted by the complete Bosanquet equation. The effective hydraulic radius therefore appears smaller than the one measured by mercury porosimetry. This will lead to a systematic error when using this observed hydraulic radius for calculations of surface free energy of the solid phase of a porous medium.

With the experimental method we use, no knowledge can be gained directly about the very initial regime of uptake due to the equilibration of the contact forces and experimental resolution over this timescale. This is the specialty of the absorption algorithm in the network simulator. At the present stage, the size of the network simulator unit cell and the computer processing time still limit direct comparison with longer term experimentation. In earlier approaches (7) a scaling function was used to extrapolate the initial regime of simulated imbibition of the unit cell where the slope of the uptake curve matches experimental data. During later stages of simulations, the boundary conditions of the unit cell, i.e. size limitations, cause a delay of liquid imbibition. In Fig. 6 we choose simulated absorption gradients of the Darcy length $\mathrm{d}x/\mathrm{d}t^{0.5}$ between 5.29 ns and 18.5 ns to compare with the experimental gradients where we have a good agreement of simulation and experimentation. Indeed it is astonishing that the mercury intrusion based network model, including the absorption algorithm, reproduces many details of the curve-shape of the experimental absorption data-based slopes.

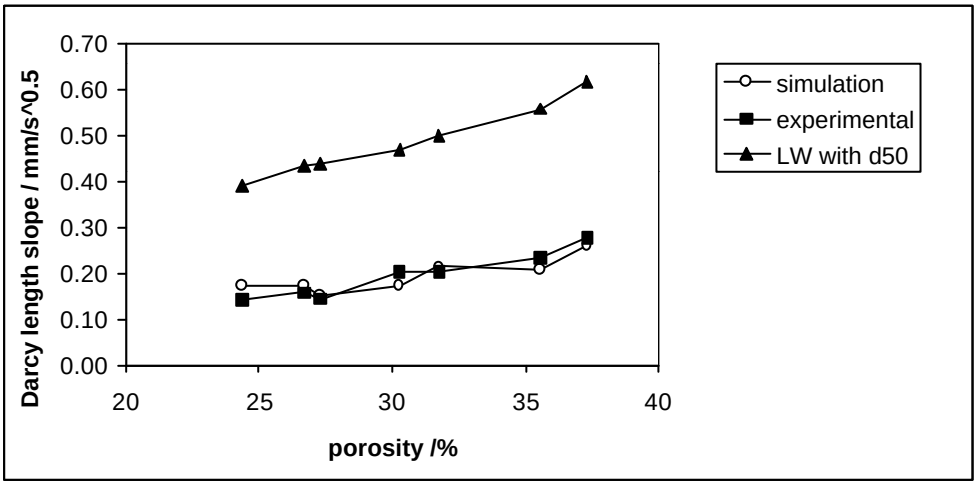

Fig. 6 *Comparison of slopes* $\mathrm{d}x/\mathrm{d}t^{0.5}$ *show at some points a very good parallel between the absorption simulation in the porosimetry data-based structure and the experimental slopes of exactly the same structures. For comparison including LW prediction from Fig. 3(b).*

ABSORPTIVE REMOVAL OF OIL FROM AN OFFSET INK

Having analyzed the absorption of pure oils the next step is to apply the technique to a commercial offset ink to detect the rate uptake of oil from the ink into the same structures using the same methodology.

Previous prediction using ink tack

Based on ISIT tack measurements in earlier work, (11), we obtained a prediction for the dynamic change in mass fraction oil content, Δf_{oil}, in a printed ink layer on a commercial offset paper. This derivation is reviewed here briefly. It is based on tack force-time integrals, $\int F(t)\mathrm{d}t$, of the individual pull-offs acting over the "pull-off" footprint area A_F, which is visible on the paper. An example of a pull-off curve is shown in Fig. 7.

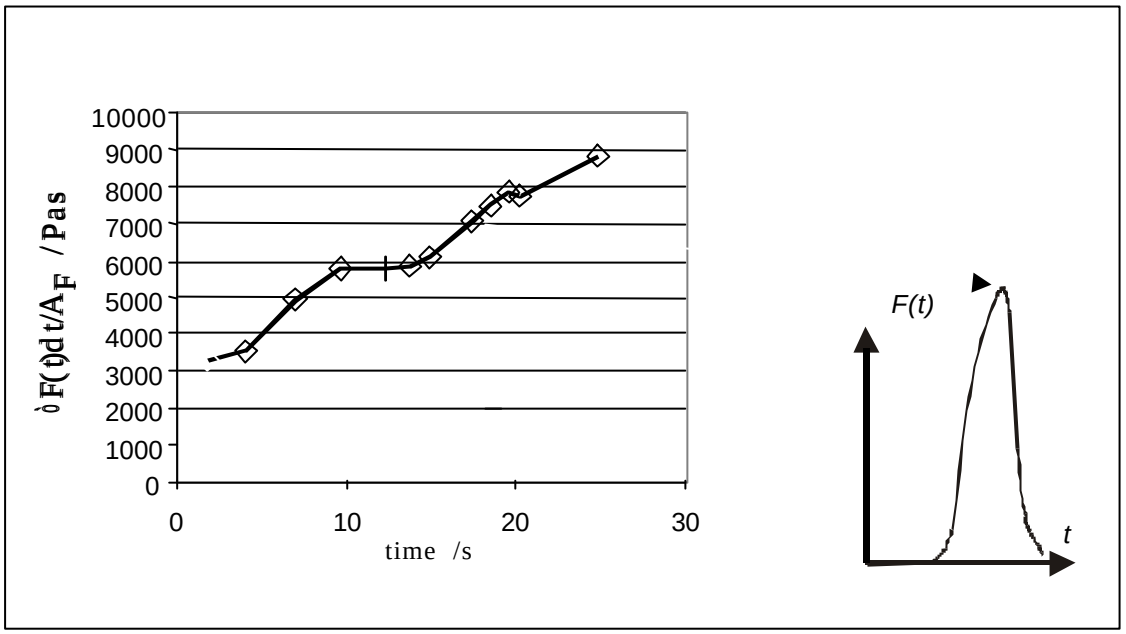

Fig. 7 *Tack rise expressed as the integrals $\int F(t)\mathrm{d}t$, of the individual pull-offs over the footprint area taken from Gane, Schoelkopf and Matthews (11).*

By using a linear extensional model for the viscosity and assuming the Trouton ratio, the following equation was derived,

$$\Delta f_{oil} \approx \frac{\ln\left(\frac{\int F(t)\mathrm{d}t}{3A_F}k\right) - a}{b} \qquad (7)$$

where k is a scaling factor, a and b are the fitting parameters from the previously determined complex viscosity after the cessation of shear $\eta^*(0)$ as a function of oil dilution. The values are plotted in Fig. 8 for the tack data of a commercial offset paper showing the time dependent decrease in oil content of the ink. Recent work from Rousu, Gane, Spielmann and Eklund (8) has shown the dominance of the preliminary absorption of mineral oil from a typical offset ink formulation, and that the removal of linseed oil is more retarded. Not knowing the formulation of our ink and the total oil makeup, we assume that at the time of 30 s, which is on the tack force plateau, the largest amount of oil removed from the setting ink is mineral-based.

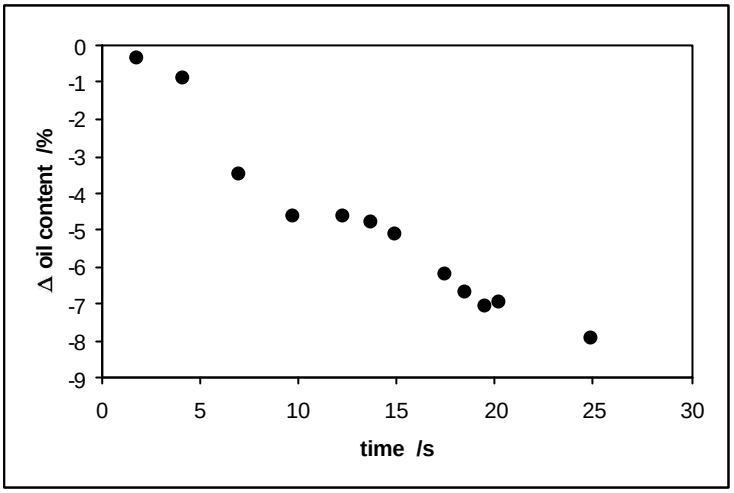

Fig. 8 *The proposed differential oil mass fraction content of the ink as a function of time in contact with the paper surface, taken from Gane, Schoelkopf and Matthews (11).*

The fraction of oil content being absorbed by the paper is decreasing linearly with time over the timescale of tack increase (Fig. 8). This linearity can be shown to be independent of the fitting parameters *a*, *b*, and the scaling parameter *k* given in Eq. 7 which only determine absolute values but not the rate order. If we assume the following linearity,

$$\Delta \phi_{oil}(t) = \phi_{oil}(t) - \phi_{oil}(0) = -ct \qquad (8)$$

where $$1/\phi_{oil}(t) = \frac{m_{oil}(t) + m_{solid}}{m_{oil}(t)} = 1 + \frac{m_{solid}}{m_{oil}(t)} \qquad (9)$$

such that, rearranging, we have the mass of oil in the ink as a function of time, $m_{oil}(t)$, in terms of the unchanging mass of solids, m_{solid}, and the original volume fraction of oil, $\phi_{oil}(0)$ in the ink, respectively.

$$m_{oil}(t) = \frac{m_{solid}}{1/\phi_{oil}(t) - 1} = \frac{m_{solid}\phi_{oil}(t)}{1 - \phi_{oil}(t)} = \frac{m_{solid}(\phi_{oil}(0) - ct)}{1 - (\phi_{oil}(0) - ct)} \qquad (10)$$

This is an interesting finding, in that absorption of free fluid over such timescales would normally have been expected to follow a $\sqrt{t}$ relationship at large *t*.

To obtain the rate of mass loss of oil, we can differentiate, to obtain,

$$\frac{dm_{oil}(t)}{dt} = \frac{-cm_{solid}}{[(1 - \phi_{oil}(0)) + ct]^2} \propto -1/t^2 \quad \text{to an approximation} \qquad (11)$$

to find that this rate falls off approximately as t^{-2}. In this case, the existence of a resistive factor forming as the ink becomes more viscous is the likely explanation.

Testing self-consistency using supersource absorption

We now extend the study by combining the pore structure modeling used for the oil absorption with the in-situ tack-based theory above to test the self-consistency of the prediction in Eq. 11 using a supersource of real ink in contact with an experimental bulk structure.

It was obvious that offset ink, showing one of the highest viscosities of all sorts of inks, could cause some severe problems of experimentation due to the low fluidity. This was confirmed after conducting a series of first experiments which led to the confused plots as shown in Fig. 9. The curves did not show any systematic behavior and were not reproducible. This forced us to analyze in some detail the phenomena arising from the high viscosity interfering with the gravimetric method.

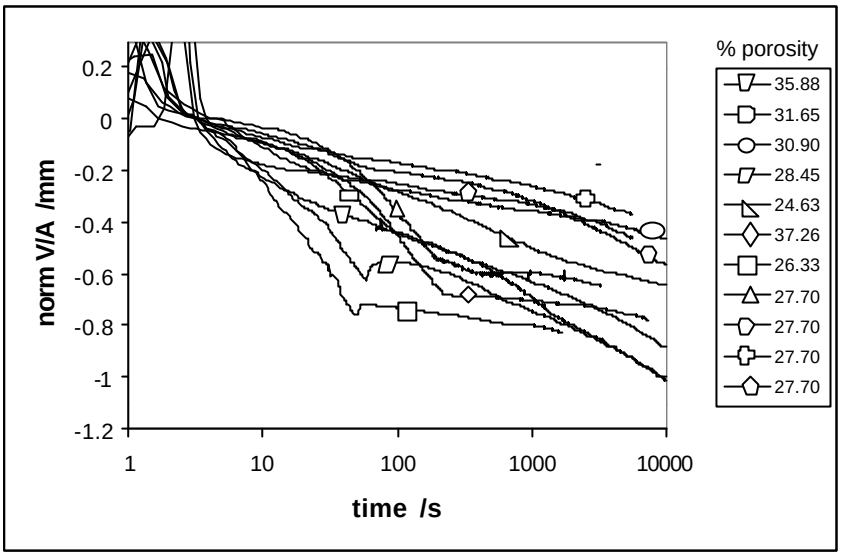

Fig. 9 *Uptake curves from the ink shown as V(t)/A normalized to [V(t=3 s) /A]=0.*

One of the curves from Fig. 9 is shown in more detail in Fig. 10. Here we see an initial upwards peak which corresponds to the sample touching the highly visco-plastic liquid. Basically, it is a mass perturbation with a viscous decay. The time for that decay is seen to be 2.5 s ± 0.2 s for the normal contacting procedure where the sample is just brought into contact with the fluid. When forcing a deeper penetration of the sample into the liquid (> 0.5 mm) the decay time increases up to 3 s. After this peak we have a regime of relatively steep decrease of weight detected by the balance, including the progressive uptake of fluid which we wish to measure, often quite abruptly going over into a regime of much lower slope. Sometimes even a short period of positive slope is observed after that point. So clearly, the regime where we would like to detect oil imbibition from the ink into the porous sample is perturbed by other phenomena which impart a force of unknown dynamics on the mass-detecting balance.

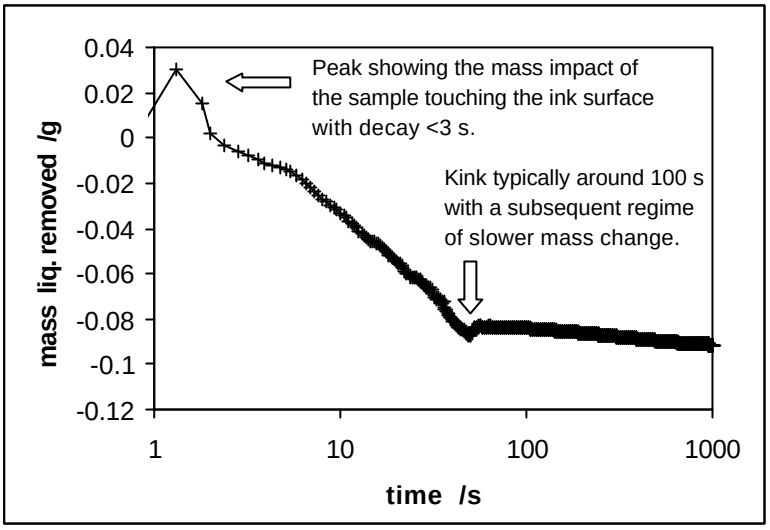

Fig. 10 *Typical curve of mass change with characteristic perturbation phenomena.*

By performing an experiment with a non absorbent cubic sample of Teflon® PTFE we analyzed the pull force of the fluid meniscus wetting the basal plane. Even when the sample is macroscopically well aligned with the ink free surface, or as perfectly as it can be with the help of the jig, there may remain some microscopical misalignment. This effect was observed earlier as a very short time phenomenon when using liquids of low and medium viscosity resulting in a constant "pull"-force. It appears now to act over a period up to 200 s in the case of the viscous ink. This effect is illustrated by an experiment highlighting the effect with the PTFE sample visibly slightly misaligned.

To overcome this misalignment effect we rounded the basal plane of the sample and performed a forced wetting, driving the sample approximately 1 mm into the fluid taking into account the strong but fast decaying pressure peak and the remaining constant buoyancy force. However, we still observed an ongoing decrease in the balance reading with the PTFE sample which could not have been absorption. Close observation of the triple interface line showed that even on the low energy PTFE, and also to be expected on the low energy silicone used for edge protection, the ink established a contact angle much smaller than 90°. Under a confocal laser scanning microscope we measured a static advancing contact angle of approximately 45°. The establishment of the contact angle toward an equilibrium force as seen on the balance lasts, in the case of PTFE, for times > 350 s. With higher energy surfaces we could expect even longer delays.

To try to solve this contact angle equilibrium problem we formed a specially shaped resin cast with a sharp edge embedding the sample as shown in Fig. 11 in order to make use of the Gibb's hinging inequality (26). The sharp edge should pin the meniscus in an approximately approached equilibrium. In practice, the edge seemed to be microscopically too round, such that there is still a considerable time of apparent mass change visible, which must still be the viscous delayed self-adjustment of the meniscus as shown in Fig. 11 to the left.

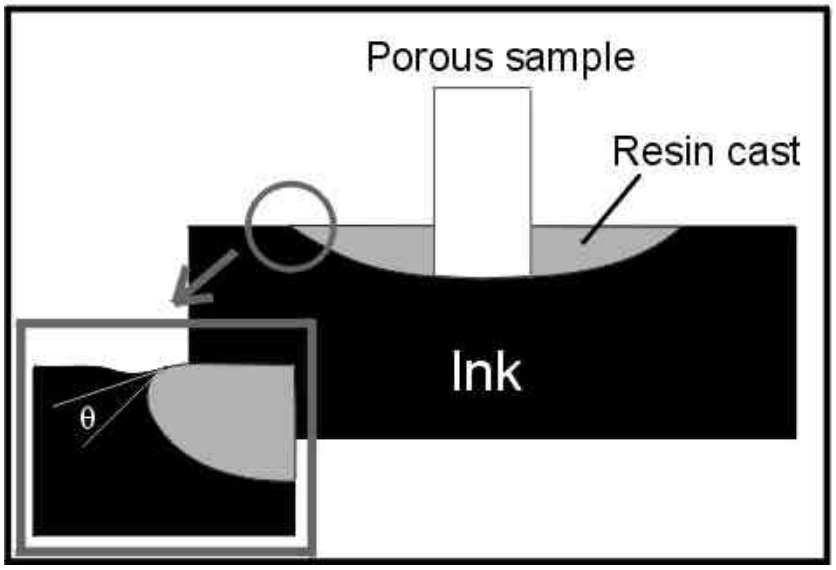

Fig. 11 *Approach attempting to make use of the Gibb's hinging inequality to try to overcome delayed meniscus formation.*

A further and final possibility was considered. A mechanical preadjustment of the contact angle, θ, could be made by consecutive immersion and retraction of the sample basal plane, gradually reducing the amplitude until an approximated equilibrium position was obtained. This is a kind of predictor / corrector method and is shown in Fig. 12. This adjustment in its present form takes too long to capture short time effects (> 50 s). However, this method gives us reasonable data for the time after the pre-adjustment. It should also be remembered that the liquid front within the structure is continually experiencing short timescale imbibition phenomena. For example, calculation shows that it takes ~ 10 ns for a 0.1 µm pore to fill (14). It can be assumed, then, that these liquid front phenomena represent the same driving force as is experienced by a thin ink layer on coated paper. Therefore, we used this curve derived from longer times for a test fit of the function type we predicted from the real time thin layer tack measurements and compared it with a Lucas-Washburn based function: compare with Equations 4, 5, 6, 10 and 11,

$$x = \sqrt{\frac{r_c \gamma_{LV} \cos\theta \, t}{2\eta}} \quad \Rightarrow \quad m_{\text{oil}}(t) = -k_2\sqrt{t} \qquad (12)$$

where k_2 is a constant containing the implicitly unknown parameters r_C, γ_{LV}, and θ. An equation of this type was given by Cameron and Bell already in 1902 (27).

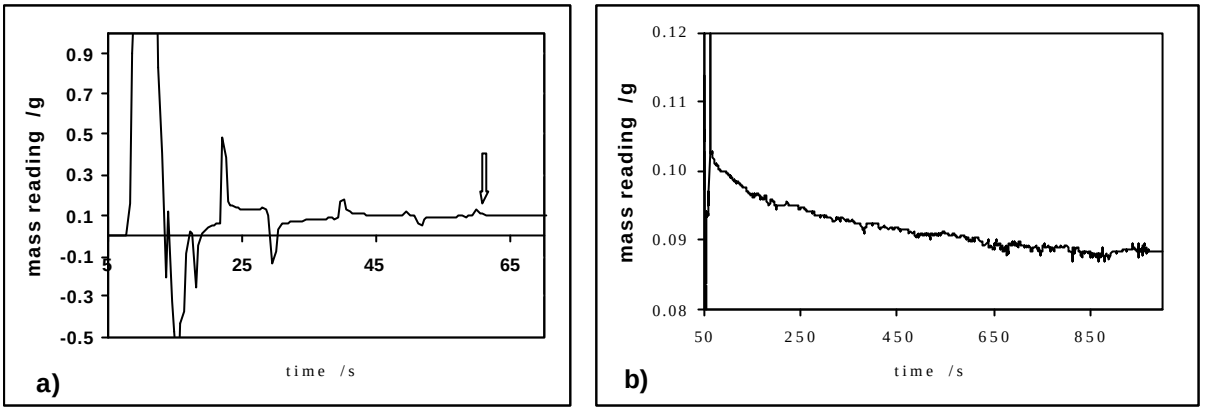

Fig. 12 *a) The preadjustment of* q*, b) the regime of absorption after the indication arrow, which is used for the extrapolative fit back to shorter time. The porosity of the sample was 26.98 %*

The difference between the prediction (Eq. 10) and the LW approach (Eq. 12) is clearly seen in Fig. 13 and confirms that it is not possible to apply a Lucas-Washburn based behavior for fluid removal from an ink (28), (29), (30), (31), (32).

The fit based on Eq. 10 gives a good correlation. This fit can be used, according to the correlation in Fig. 13, to consider timescales shorter than those which can be captured by our supersource experiment. Furthermore, we recall that, on a printing press, thin layers of printing ink are applied to relatively thin layers of coating. A typical ratio might be ~1 µm of ink thickness, for a four color full-tone print, compared with 4-10 µm of coating. Since coatings have ~< 25 % porosity, the lower range of coating thicknesses can become saturated, i.e. supersource conditions can occur in printing, especially when one considers the additional dilution by fountain solution. That the fitted solution to Fig. 13 matches that which was derived from completely independent measurements of ink tack development on paper tends to support the relevance of this claim.

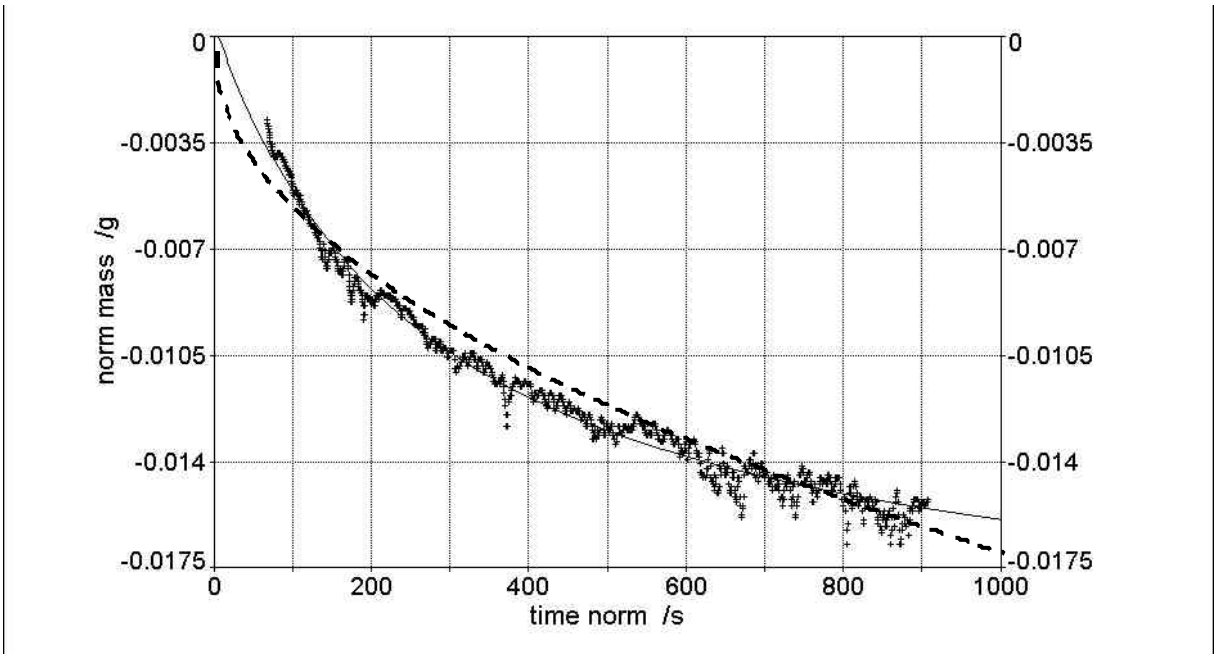

Fig. 13 *Comparison of a fit based on "our" predicted Eq. 10 (full line) and a fit of Eq.12, Washburn-type (dashed line). The fitting parameters are given in the appendix.*

The dependent mass axis in Fig. 13, which was based on a relative starting absorption mass, was shifted to fulfill the boundary condition $m_{oil}(0)=0$, stating that no oil was lost at time $t=0$, where $t=0$ is the start of the experiment at the first point of contact between sample and ink. It is not possible with this experimentation to get data for the individual $t=0$ factors in Eq. 10, but our target was achieved in that we wished to test the proposed general rate behavior from Eq. 11.

The result of this analysis means in physical terms that the absorption relationship is *not* dependent on a square root time law. We see that the case of supersource imbibition rate corresponds to the thin film application of the ISIT as measured during tack rise. Therefore, the continuity of the fluid in contact must be maintained similarly in both cases. The concept of a delineated filtercake action was seen as unlikely during this time period at least (11), rather the observation supports a continuous increasing concentration gradient toward the sample or paper boundary in the case of an offset ink. We can confirm here that the ISIT during tack rise samples the viscosity and solids content of the complete ink layer irrespective of any effective longer term boundary structure formation. We have, therefore, not corrected for the effect of buoyancy of a distinctly forming filtercake, i.e. immobilized ink, in the gravimetric experiment, in contrast to the approach used when considering a much more mobile flexographic ink (10) where a filtercake structure had been clearly observed.

CONCLUSIONS

The dynamic of oil absorption from an ink has been shown to be different from that of pure oil. The dynamic absorption of oil from an offset ink into a porous paper coating structure from a super source, i.e. the case of abundant ink in contact with a porous block of coating pigment, is shown to be the same as in thin layer application (printing) during the early stages of absorption from that layer. This was confirmed by fitting the dynamic equation derived directly from tack and ink viscosity measurements, applying to thin films, to that of experimental super source imbibition. The determination, therefore, of ink solids and viscosity, made using the static position ink tack force-time integral of the Ink Surface Interaction test method (ISIT), has now been supported in terms of super source rate predictions. The concentration gradient continuity of the fluid ink in contact with the porous substrate is therefore expected to be maintained in both cases. The *mass fraction of oil* lost from the ink follows a linear t absorption rate. The *absolute mass absorption* of the oil into the coating is *not* linear t related but decays approximately according to $\sim 1/t^2$. The initial ink tack rise dynamic cannot, therefore, be predicted by Lucas-Washburn, and it is misleading to refer to a Darcy absorption length in a porous medium containing a distribution of interconnecting pore sizes due to the previously observed phenomenon of selectively unfilled pores. This is modeled as an absorption dynamic related to a sequential inertial imbibition selection acting initially to exclude portions within a porous network structure favoring the progress of fluid through the finer pores which then subsequently follow the expected viscous retardation.

APPENDIX

Eq. 10 is reduced to the form $\Rightarrow y = a + \left(\frac{b(c-dx)}{1-(c-dx)} \right)$, and the fit to the absorption curve provides values of,

a=11.435, b= 11.456, c=-533.113, d= 2.162, r^2=0.986, FitStdErr=0.000417

Eq. 12 is reduced to the form $\Rightarrow y = a + b\sqrt{x}$, and the fit to the absorption curve provides values of,

a=0.0005327, b= -0.0005528, r^2= 0.966, FitStdErr=0.000637

The software for MS Windows™ used for the balance data sampling was developed by Dr. D.C. Spielmann of Omya AG and may be requested at daniel.spielmann@omya.com.

REFERENCES

1. Gane, P. A. C., Schoelkopf, J., Spielmann, D. C., Matthews, G. P., and Ridgway, C. J., "*Observing fluid transport into porous coating structures: some novel findings*", Tappi Advanced Coating Fundamentals Symposium April 29-May 1, Toronto, Canada, Sheraton Centre, Tappi Press, 1999, p213-236

2. Bosanquet, C. H., "*On the flow of liquids into capillary tubes*", Philosophical Magazine, 1923, p525-531

3. Washburn, E. W., "*The dynamics of capillary flow*", The physical review, XVII(3), 1921, p273-283

4. Schoelkopf, J., Gane, P. A. C., Ridgway, C. J., and Matthews, G. P., "*Influence of inertia on liquid absorption into paper coating structures*", Paper and Coating Chemistry Symposium, Stockholm, Sweden2000, p422-430

5. Bernadiner, M. G., "*A capillary microstructure of the wetting front*", Transport in Porous Media, 30(1998, p251-265

6. Quere, D., "*Inertial capillarity*", Europhysics Letters, 39(5), 1997, p533-538

7. Schoelkopf, J., Ridgway, C. J., Gane, P. A. C., Matthews, G. P., and Spielmann, D. C., "*Measurement and network modeling of liquid permeation into compacted mineral blocks*", Journal of Colloid and Interface Science, 227(2000, p119-131

8. Rousu, S. M., Gane, P. A. C., Spielmann, D. C., and Eklund, D., "*Separation of off-set ink components during absorption into pigment coating structures*", Paper and Coating Chemistry Symposium 2000, Stockholm, Sweden2000, p527-553

9. Xiang, Y. and Bousfield, D. W., "*The influence of coating structure on ink tack development*", PanPacific and International Printing and Graphic Arts Conference, CPPA, 1998, p93-101

10. Gane, P. A. C. and Ridgway, C. J., "*Absorption rate studies of flexographic ink into porous structures: relation to dynamic polymer entrapment during preferred pathway imbibition*", 27th IARIGAI Research Conference, Advances in Paper and Board Performance, Graz, Austria, 2000

11. Gane, P. A. C., Schoelkopf, J., and Matthews, G. P., "*Coating imbibition rate studies of offset inks: a novel determination of ink-on-paper viscosity and solids concentration using the ink tack force-time integral*.", 2000 International Printing and Graphic Arts, October 1-4, 2000, Hyatt Regency Savannah, Georgia, Tappi Press, 2000, p71-88

12. Gane, P. A. C., Kettle, John P., Matthews, G. Peter, and Ridgway, Cathy J., "*Void space structure of compressible polymer spheres and consolidated calcium carbonate paper-coating formulations*", Industrial and Engineering Chemistry Research, 35(5), 1996, p1753-1764

13. Oittinen, Pirkko, "*Fundamental rheological properties and tack of printing inks and their influence on ink behaviour in a printing nip*", 1976, Thesis, Helsinki Unisversity of Technology, Finland

14. Schoelkopf, J., Ridgway, C. J., Gane, P. A. C., Matthews, G. P., and Spielmann, D. C, "*Measurement and network modelling of liquid permeation into compacted mineral blocks*", Journal of Colloid and Interface Science, 227(2000, p119-131

15. Matthews, G. P., Ridgway, C. J., and Small, J. S., "*Modelling of simulated clay precipitation within reservoir sandstones*", Marine and Petroleum Geology, 13(5), 1996, p581-589

16. Ridgway, C. J., Ridgway, K., and Matthews, G. P., "*Modelling of the Void Space of Tablets Compacted over a Range of Pressures*", Journal of Pharmacy and Pharmacology, 49, 1997, p377-383

17. Peat, D. M. W., Matthews, G. P., Worsfold, P. J., and Jarvis, S. C., "*Simulation of water retention and hydraulic conductivity in soil using a three-dimensional network*", European Journal of Soil Science, March 2000, p65-79

18. Matthews, G. P., Ridgway, C. J., and Spearing, M. C., "*Void space modeling of mercury intrusion hysteresis in sandstone, paper coating, and other porous media*", Journal of Colloid and Interface Science, 171(1), 1995, p8-27

19. Ridgway, C. J., Schoelkopf, J., Matthews, G. P., Gane, P. A. C., and James, P. W., "*The effects of void geometry and contact angle on the absorption of liquids into porous calcium carbonate structures*", Journal of Colloid and Interface Science, 239(2), 2001, p417-431

20. Chibowski, E. and Holysz, L., "*On the use of Washburn's equation for contact angle determination*", Journal of Adhesion Science and Technology, 10, 1997, p1289-1301

21. Holysz, L. and Chibowski, E., "*Surface free energy components of calcium carbonate and their changes due to radiofrequency electric field treatment*", Journal of Colloid and Interface Science, 164, 1994, p245-251

22. Yang, Y.-W. and Zografi, G., "*Use of the Washburn-Rideal equation for studying capillary flow in porous media*", Journal of Pharmaceutical Sciences, 75(7), 1986, p719-721

23. Li, Z., Giese, R. F., van Oss, C. J., Kerch, H. M., and Burdette, H. E., "*Wicking technique for determination of pore size in ceramic materials*", Journal of American Ceramic Society, 77(8), 1994, p2220-2222

24. Marmur, A. and Cohen, R. D., "*Characterization of porous media by the kinetics of liquid penetration: the vertical capillaries model*", Journal of Colloid and Interface Science, 189, 1997, p299-304

25. Chibowski, E., "*Solid surface free energy components determination by the thin-layer wicking technique*", Journal of Adhesion Science and Technology, 6(9), 1992, p1069-1090

26. Kent, H. J. and Lyne, M. B., "*Influence of paper morphology on short term wetting and sorption phenomena*", Fundamentals of Paper Making, Mechanical Engineering Publications Limited, London, 1989, p895-920

27. Bell, J. M. and Cameron, F. K., "*The flow of liquids through capillary spaces*", Journal of Physical Chemistry, 10, 1906, p658-674

28. Xiang, Y. and Bousfield, D. W., "*The influence of coating structure on ink tack development*", Printing and Graphic Arts Conference, 6 - 8 October), 1998, p93-101

29. Preston, J. S., Elton, N. J., Legrix, A., and Nutbeem, C., "*The role of pore density in the setting of offset printing ink on coated paper*", 2001 Advanced Coating Fundamentals Symposium Proceedings, Tappi, San Diego, California USA, 2001, p21-50

30. Leskinen, A. M., "*Influence of the paper on the evaporative drying of inks*", The Finnish Pulp and Paper Research Institute, Finland, 1986, p381-398

31. Nederveen, C. J., "*Absorption of liquid in highly porous nonwovens*", Tappi Journal, 77, 1994, p174-180

32. Lepoutre, P., "*Liquid absorption and coating porosity*", Paper Technology and Industry, 1978, p298-304